Print
2 copies

MAY 1972

MDC G3144

FEASIBILITY STUDY OF OXYGEN-DISPENSING EMITTERS FOR THERMIONIC CONVERTERS

PHASE I-FINAL REPORT

by
J. G. DeSteese

Prepared Under Contract No. 953125 by
Donald W. Douglas Laboratories
McDonnell Douglas Astronautics Company
for
JET PROPULSION LABORATORY

PREFACE

This document is the Phase I Final Report submitted by the Donald W. Douglas Laboratories, Richland, Washington, under Contract No. 953125, and covers the period from 23 June 1971 through 15 April 1972.

This program is being monitored by the Jet Propulsion Laboratory, Pasadena, California, for the National Aeronautics and Space Administration. Dr. K. Shimada is the Technical Monitor for the program.

This work was performed for the Jet Propulsion Laboratory, California Institute of Technology, sponsored by the National Aeronautics and Space Administration under Contract NAS7-100.

CONTENTS

FIGURES

TABLES

SUMMARY

A metal/ceramic Marchuk tube was used to measure work functions of oxygen-doped tantalum, to determine applicability of the material to plasma-mode thermionic converters. Oxygen-doped tantalum was shown to increase in work function monotonically with oxygen doping in the range 0.1 to 0.3 atomic percent (a/o).

Bare work function data taken at $T/T_{Cs} > 4$ were extrapolated according to the Rasor-Warner cesium adsorption model to the region $T/T_{Cs} \sim 3$. Using this extrapolation, the program goal of work function reduction was achieved with oxygen doping in the range 0.2 to 0.3 a/o.

Oxygenated test emitters were run at an average temperature of 2165°K and a T/T_{Cs} ratio ~5.8 to observe the influence of oxygen depletion. Bare work function decreased with outgassing of oxygen. Projections were made based on outgassing kinetics and area/volume ratios to calculate the longevity of oxygen doping in a practical converter. Calculations indicated that the program goal of 3.6×10^7 seconds (10,000 hr) could be achieved at 1800°K with an initial oxygen doping of 1 a/o and a practical emitter area/volume ratio.

Section 1
INTRODUCTION

In the past decade, several techniques have been developed for preparing emitter surfaces to allow operation at practical electrode spacings in thermionic direct energy conversion devices. In all converters containing cesium, a major design goal is to obtain suitable electrode properties at the lowest possible cesium pressure. Reduced cesium pressure tends to minimize the irreversible vapor conduction loss component of the emitter thermal balance in all modes of operation. In the plasma discharge mode, the product of cesium pressure p(torr) and electrode spacing d(mil) is an important indication of optimum converter performance. The operating point for the ignited and unignited mode is pd $\sim$20 $\pm$10 torr-mil and pd $\sim$ 3 $\pm$1 torr-mil, respectively. In both discharge modes, a reduction in pressure can be accompanied by a larger and therefore more practical electrode spacing to maintain the pd product in the optimum range.

The fundamental approach to modifying emitter surfaces has been selecting and treating materials to provide a cesiated work function characteristic occuring at high surface-to-cesium-reservoir temperature ratios (T/T_{Cs}) on the Rasor-Warner diagram (Reference 1). Several techniques for producing the desired emitter modification are reported in the literature. Examples of basic approaches to emitter treatment are presented in References 2 through 6. However, emitter modification are generally classified in two categories:

1. Surface orientation to expose high bare-work function crystal structure (Reference 2).
2. Exposure of the cesiated surface to electronegative additives.

Treatments in the second category include oxygen supplied to the surface in either gaseous or cesium compound form (References 3 and 4), pre-treatment of the surface to achieve an active atomic oxygen monolayer (Reference 5), and oxygen dissolution in the bulk electrode material (Reference 6).

In practical converters, it is important that emitter treatment be stable throughout the operating lifetime. However, there are several potential disadvantages with most emitter-treatment techniques. Preferred crystal orientation in the surface is susceptible to long-term degradation by diffusion and thermal etching. A surface atomic layer may suffer irreparable degradation if the surface active element is removed by impurity reactions during the converter life. Finally, converter operation which depends on an additive supply from an external reservoir, while not as susceptible to degradation as the surface monolayer system, suffers from the inconvenience imposed by the requirement to maintain separate cesium and additive reservoirs. The beneficial additive effect obtained by dissolution of oxygen in cesiated tantalum has been recognized for some time (Reference 7) and has shown long-term stable electrode operation in the ISOMITE® battery development program (Reference 6). The oxygen component in the Ta-O-Cs surface system appears to be supplied from bulk Ta-O solid solution. Electrode surface corrosion may, therefore, tend to be repaired by diffusion of oxygen to the electrode surface. This oxygen dispensation process appears to provide a reliable and reproducible controlled reservoir for an electronegative surface additive.

Experience to date with the Ta-O-Cs electrode system has been restricted to Isomite converters operating in the quasi-vacuum mode. A principal distinction between these converters and conventional thermionic devices is the use of low emitter temperatures (900° to 1400°K) and low cesium vapor pressures (10^{-3} to 10^{-1} torr). Low temperature and low cesium vapor pressure tend inherently to minimize degradation of the Ta-O-Cs surface system. DWDL experience shows that electrodes containing less than 1 atomic percent (a/o) of oxygen are stable in excess of 36,000 hours a typical Isomite temperatures. The successful use of oxygenated electrodes in quasi-vacuum-mode devices and the retention of oxygen by tantalum after extreme outgassing (Reference 8) suggests that the solid-solution Ta-O dispensing reservoir may be applicable to high-temperature conventional converters.

PROGRAM OBJECTIVES

The objective of this program is to define the quantity of absorbed oxygen required to produce a stable and useful surface modification in cesiated tantalum emitters. In quantitative terms, a definition is required of the amount of oxygen doping in tantalum to yield the following:

1. Cesiated work functions which are approximately 0.3 ev lower than that of pure tantalum at the temperature ratio $T/T_{Cs} \sim 3$.
2. Emitters which are continuously operable at 1800°K in excess of 10,000 hours without entirely depleting the absorbed oxygen.

PROGRAM STRUCTURE

The feasibility study of oxygen-dispensing tantalum involves the use of simple wire-loop test emitters exposed to cesium vapor in a Marchuk-type plasma-anode tube (Reference 9). Phase I of program consists of five principal tasks:

Task 1 - Fabricate three tantalum test electrodes.

Task 2 - Fabricate one reference electrode.

Task 3 - Prepare Marchuk plasma-immersion tube, install test emitters, and cesiate the assembly.

Task 4 - Measure work functions of cesiated test emitters.

Task 5 - Measure oxygen depletion rate at high electrode temperature.

In Task 1, three tantalum test electrodes containing different quantities of absorbed oxygen were constructed in a configuration suitable for insertion into a JPL-supplied Marchuk tube. The tantalum electrode to be constructed in Task 2 provides a reference test emitter for comparison with test results from the doped tantalum electrodes. Task 3 involves preparation of the plasma anode tube and installation of test emitters followed by a high temperature bakeout and cesiation. Measurement of the cesiated work function characteristic and oxygen depletion rate of each electrode are accomplished in Tasks 4 and 5 respectively.

The following sections describe experimental techniques, results and recommendations for probe modifications to be used in the Phase II and Phase III programs.

Section 2
PHASE I EXPERIMENTAL APPROACH

The Phase I experimental approach was based on use of a JPL-supplied Marchuk tube. Shimada and Cassell (Reference 10) have described its construction and operation in argon. This tube is a metal/ceramic assembly designed to exceed the range of operating capabilities normally associated with the conventional glass envelope configuration (Reference 7, 8, 9, and 11). Metal/ceramic construction permits increased current-carrying capacity and leadthrough resistance to cesium corrosion, as well as high bake out (700°K) and operating temperature, and demountable electrodes. Tantalum wire test emitters doped with nominally 0.1, and 0.2, and 0.3 atomic percent (a/o) of oxygen were prepared and mounted in the Marchuk tube. Emission measurements were made in cesium vapor and compared with emission characteristics of a rigorously outgassed, but undoped tantalum reference electrode. Oxygen-doping was achieved by aqueous anodization of the tantalum wires and subsequent dissolution of the anodic film in the tantalum substrate.

This section contains a detailed summary of construction and preparation techniques used in this effort.

OUTGASSING OF TANTALUM

Four certified-purity (Appendix A) 0.254-mm (10-mil) diameter tantalum wires were ultrasonically cleaned in reagent-grade ethyl alcohol, suspended in a Vac Ion high-vacuum system (Model No. 933-0005), and outgassed to provide a reference condition prior to oxygen doping. Samples approximately 30-cm long were outgassed sequentially for 3600 seconds between 2400° and 2500°K, observed with a residual 1.33×10^{-7} N/m^2 (1×10^{-9} torr) pressure indicated by the Vac-Ion pump current. Figure 2-1 shows the configuration of the wires during this procedure. Each wire was flashed seven times and accumulated approximately 600 seconds at 2800°K.

71-1508

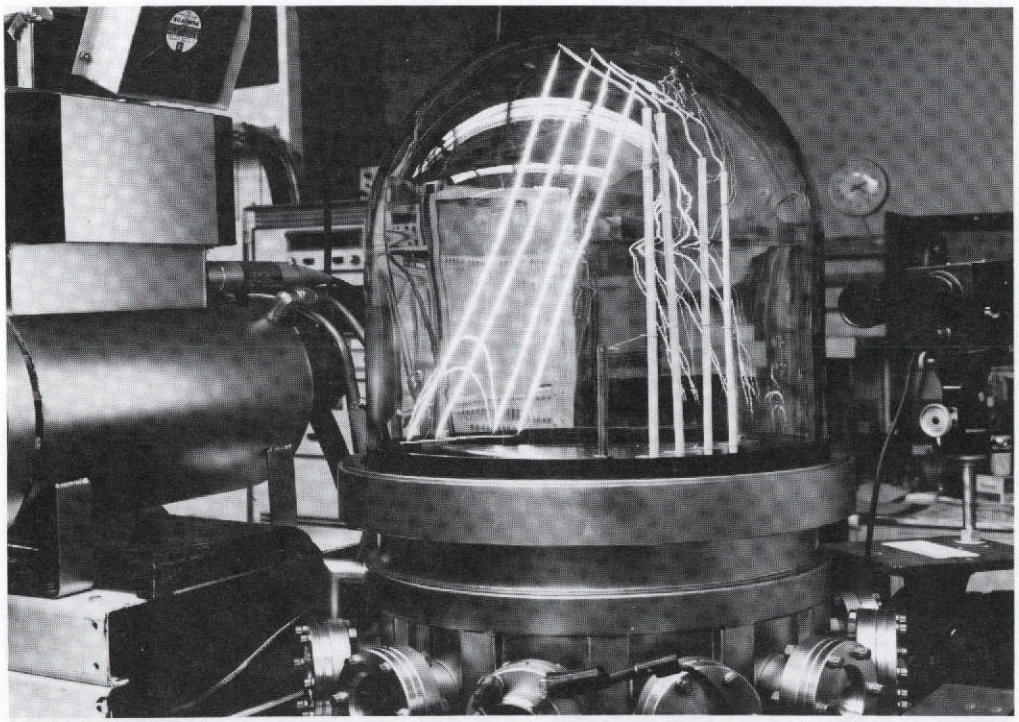

Figure 2-1. Ta Wire Outgassing

During final outgassing, pump current indicated a pressure less than 1.33×10^{-6} N/m^2 (10^{-8} torr). The wires were cooled to room temperature, then heated cyclically to approximately 1000°K. Surface adsorbed gas was observed as a brief transient pressure increase and was essentially reproducible as a function of time between temperature cycles. The gas burst was attributable to surface adsorbed materials contributed by the equilibrium 10^{-7} N/m^2 ($\sim 10^{-9}$ torr) residual atmosphere.

Wire temperature was measured by an Epic micropyrometer (Model No. 3318) calibrated using an NBS-traceable standard. A correction for the bell jar transmissivity was included in the calibration. The correlation between brightness temperature and true temperature was derived from thermal emissivity data in Reference 12. During outgassing, a transparent tantalum film was deposited on the bell jar. A transmissivity measurement was run on this film after processing the wires. The error introduced by the condensation of tantalum averaged about 20°K in measuring brightness temperature. This was considered an insignificant perturbation.

Outgassing was chosen to produce a wire-sample reference condition with a significantly lower residual oxygen concentration (<0.01 a/o) than achievable by anodic doping. To avoid excessive vaporization and grain growth leading to mechanical failure of the wires, the vaporization rate of tantalum was calculated from vapor pressure data in Reference 13. The thermal treatment removed less than 5 μm from the wire diameter, which was substantiated by measuring samples before and after treatment.

Calculations reported by Gebhardt, et al (Reference 14) show residual oxygen in 0.02-mm (8-mil) tantalum sheet has a half life of 2.3×10^{-2} second at 2673°K. The outgassing of wires in this program should therefore provide an acceptably low residual oxygen content. One of the four wires was used without further treatment to fabricate the reference test emitter.

ANODIZATION OF TANTALUM

A literature survey was performed to review known oxidation and anodizing characteristics of tantalum. Most of the reviewed literature is listed in Section 5. The remainder is listed in Section 6.

Several methods are available for anodizing tantalum, including heating in oxygen, reactive sputtering, rf glow discharge, and aqueous techniques. Heating in oxygen requires meticulous care in controlling impurities, and both sputtering and rf glow discharge methods suffer from a non-ideal electronic conversion efficiency (i.e., each electron received by the surface is not utilized in the formation of an oxide). Worledge and White (Reference 15) report about 70% electronic efficiency for the glow discharge, and Vratny (Reference 16) describes poor electrical characteristics and significant non-uniformities in the oxide film produced by reactive sputtering.

Aqueous anodizing appears to be the preferred technique for producing oxide films on tantalum. Amsel, et al (Reference 17) report electronic efficiencies greater than 99% in aqueous salt solutions and dilute (approximately 1%) acids. Moreover, uniformity within 1% to 4% is commonly expected by aqueous anodizing. The major questions concerning aqueous anodizing are film purity and deposition rate. In a series of experiments, Randall et al (Reference 18) demonstrated by a radioactive tracer technique, that oxygen

appears to come almost solely from the water, rather than from the acid or salt. They showed that acid concentrations over 50% are necessary before any impurity ions are detected in the film.

In this program, tantalum was anodized in a 0.01 molar HNO_3 solution at 293°K, with a current density of 1 ma/cm^2. Three of the four outgassed wires were anodized to respectively provide 0.1, 0.2, and 0.3 a/o oxygen in solid solution with tantalum after the films were dissolved into the wire substrate. For each sample, a film thickness was calculated assuming a Ta_2O_5 layer with a density of 8.74 g/cm^3, to provide the appropriate Ta/O atomic ratio.

The wires were anodized inside a cylindrical tantalum electrode, positioned on the cylindrical axis to ensure a uniform current density. A previously anodized tantalum weight held each wire taut and parallel to the cylindrical axis. The weight was anodized and insulated from the wire with a small alumina ring to prevent interference with the surface current density on the wire sample.

The thickness of each film was indicated by the potential across the cell. According to Amsel, et al, the rate of change in film thickness (dx/dt) can be expressed in terms of the electric field (E) across the film and the rate of change in cell voltage (dv/dt), by

$$\frac{dx}{dt} = \frac{1}{E} \frac{dv}{dt} \tag{2-1}$$

The electric field is related to the ionic current density (J_{ox}) by

$$E = \frac{1}{\beta} \ln \left(\frac{J_{ox}}{\alpha}\right) \tag{2-2}$$

where α and β are tantalum oxidation constants. Combining equations (2-1 and 2-2) the rate of change in anodic film thickness with voltage (dx/dv) is given by

$$\frac{dx}{dv} = \frac{1}{\frac{1}{\beta} \ln \frac{J_{ox}}{\alpha}} \tag{2-3}$$

Using values for α and β determined by Vermilyea (Reference 19) for oxidation in aqueous media

$$\frac{dx}{dv} = 1.56 \text{ nanometers per volt} \qquad (2\text{-}4)$$

Table 2-1 summarized the film thickness and cell voltage for each level of oxygen doping.

Table 2-1
ANODIC FILM THICKNESS AND VOLTAGE

Oxygen Doping (a/o)	Calculated Film Thickness (nm)	Voltage (v)
0.1	59	38
0.2	118	76
0.3	177	114

Film thickness was verified using a Millis Research Model CSG-18 Color Step Gage. Attempts were also made to correlate the hardness and lattice parameter of the tantalum/oxygen solid solutions with values in the literature; these results are discussed in Section 3. At the doping levels achieved in this program, both chemical techniques and neutron activation analysis require larger samples than were available to reach the detection limit for oxygen. For example, to detect an oxygen doping of 0.1 a/o, a tantalum wire 1.75 m long is required. It was found to be physically impractical to prepare specimens of this length and provide the required uniformity of outgassing and anodizing.

DIFFUSION OF OXYGEN IN TANTALUM

After anodizing, three tantalum wires were remounted in the vacuum system shown in Figure 2-1 and electrically heated to dissolve the Ta_2O_5 layers into the tantalum-wire substrate. A vacuum of 10^{-7} N/m^2 ($\sim 10^{-9}$ torr) was established with the samples at room temperature. Oxygen diffusion in tantalum was treated analytically (Appendix B) to establish time and temperature relationships for the diffusion process. Theoretical diffusion profiles

for 1073°, 1273°, and 1473°K are shown in Figures 2-2, 2-3, and 2-4. Diffusion profiles were derived by Fourier series solution to the diffusion equation in Appendix B, using diffusion coefficient data for oxygen in tantalum from Reference 20. A slab geometry is amenable to analysis and yields a conservative time/temperature estimate for wires equal in diameter to the slab thickness. Figure 2-3 shows elimination of oxygen concentration gradients after approximately 3 hours at 1273°K. To minimize sublimation of tantalum-oxide species, the wires were heated to approximately 900°K until the characteristic color of the anodic film disappeared. Temperatures were then increased to 1273°K and maintained for 10^4 seconds. After heating, the wires had a metallic luster over a major portion of the length. Traces of film color were apparent within to 1.5 cm of each end where the wires were spot-welded to the support structure.

TEST EMITTER CONSTRUCTION (TASK 1 AND 2)

Test emitter were constructed from the central portion of each processed wire and, in no case, was material taken nearer than 5 cm from the supported ends. Figure 2-5 shows a typical emitter mounted on a Varian flange. Nickel leads were connected to the ends of the test emitter loop and shielded by nesting ceramic tubes to within 1.5 cm of the flange. Two guard rings protecting the junction of the ceramics were connected to a third nickel lead. The nickel leads were brazed into Alberox type CT-250 metal/ceramic leadthrough assemblies. The ceramic sleeves on each emitter were fired in a 10^{-4} N/m^2 ($\sim 10^{-6}$ torr) vacuum at 1800°K for 1 hour before assembly.

The length of each emitter was determined to the required accuracy (±2.5%) by measuring loop length in an approximately 10x enlargement photograph. Copper wires were bent to conform to the enlarged probe images and knife edge witness marks were made at the points of emergence from the ceramic sleeves. The copper wires were straightened and the distance between marks measured with a vernier caliper. The scale of the photographs was determined by the ratio of apparent diameter to actual wire diameter measured with a precision micrometer.

Maximum error contributed by this method was 0.25 mm in the length of the enlarged photograph. This corresponds to approximately 0.03 mm error in

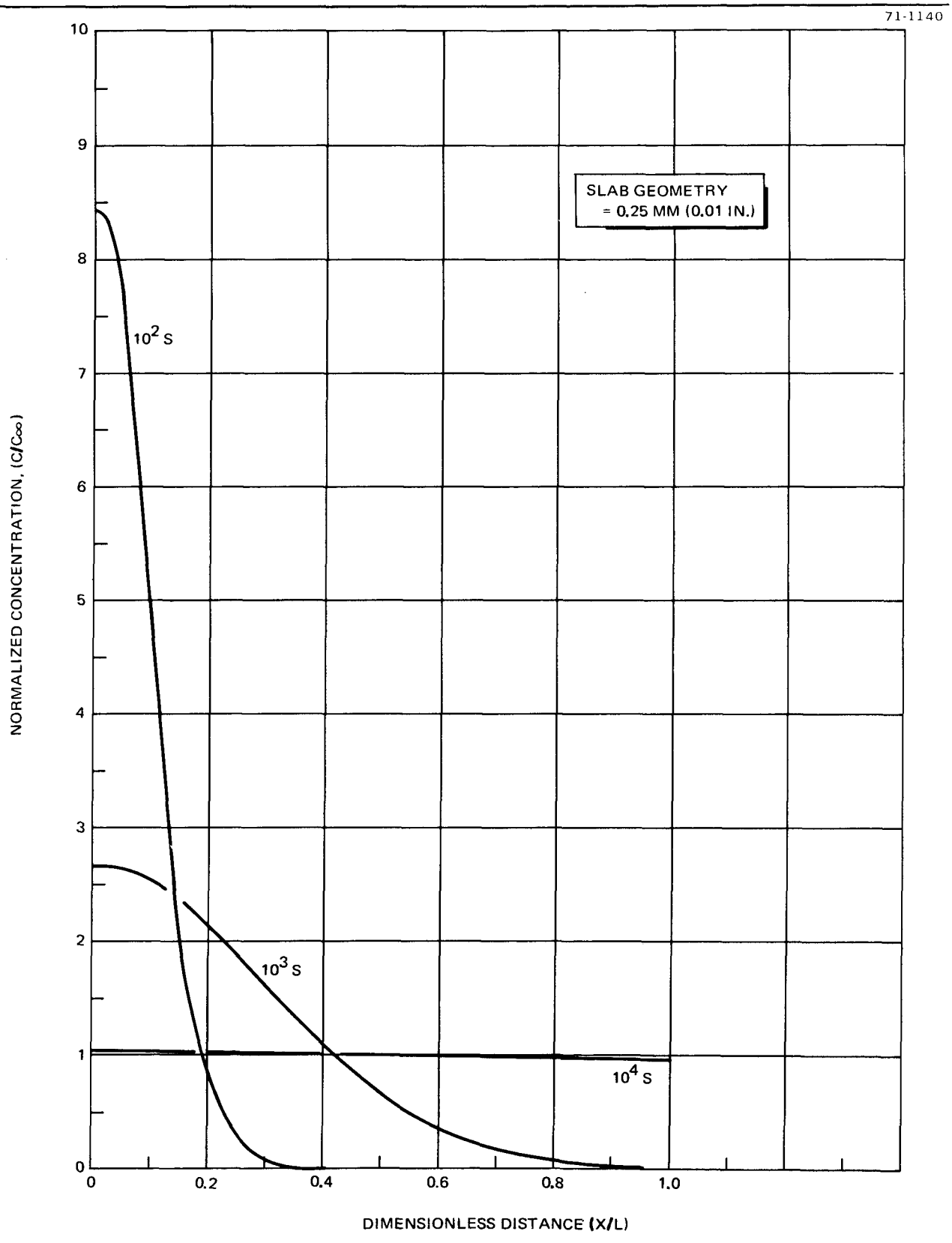

Figure 2-2. Theoretical Diffusion Profiles of Oxygen in Tantalum at 1073°K

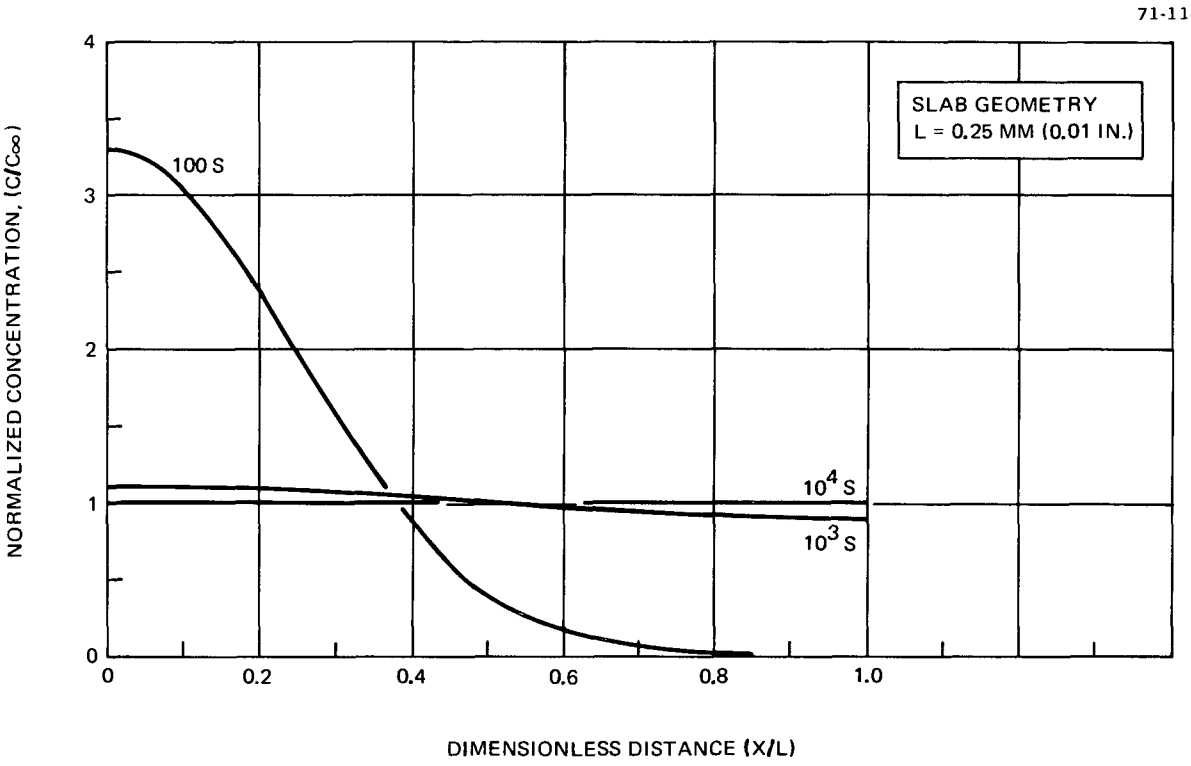

Figure 2-3. Theoretical Diffusion Profiles of Oxygen in Tantalum at 1273°K

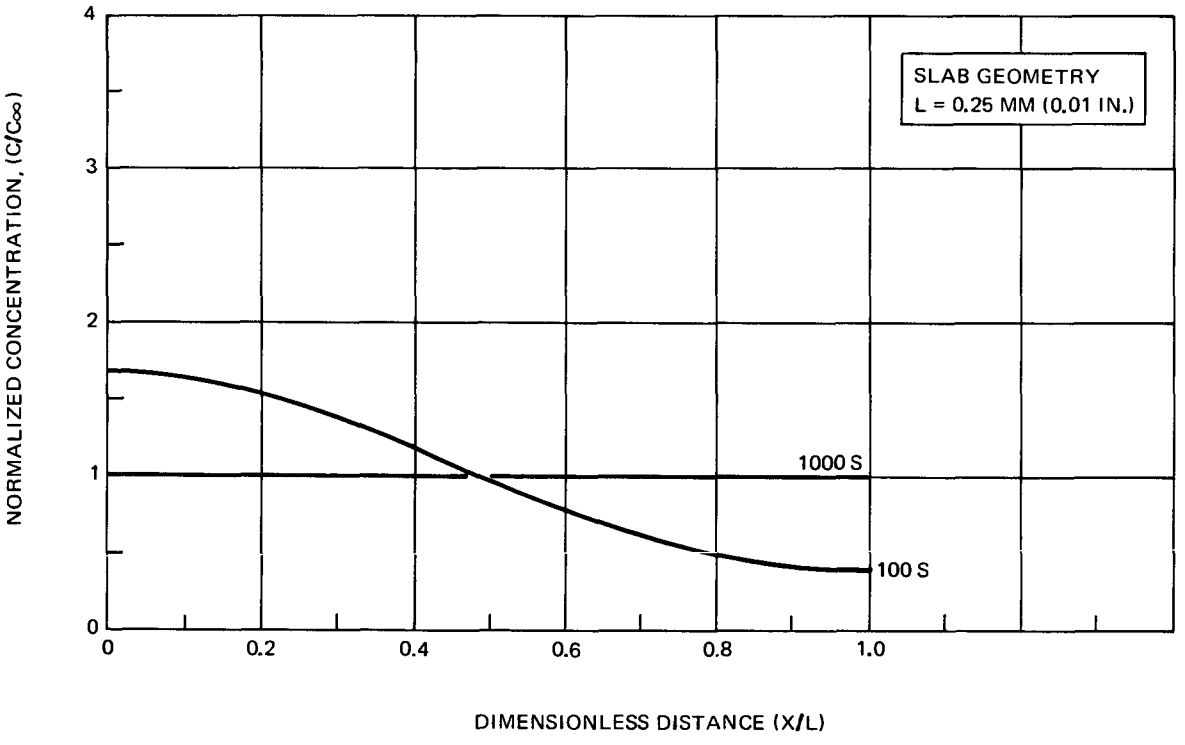

Figure 2-4. Theoretical Diffusion Profiles of Oxygen in Tantalum at 1473°K

71-1649

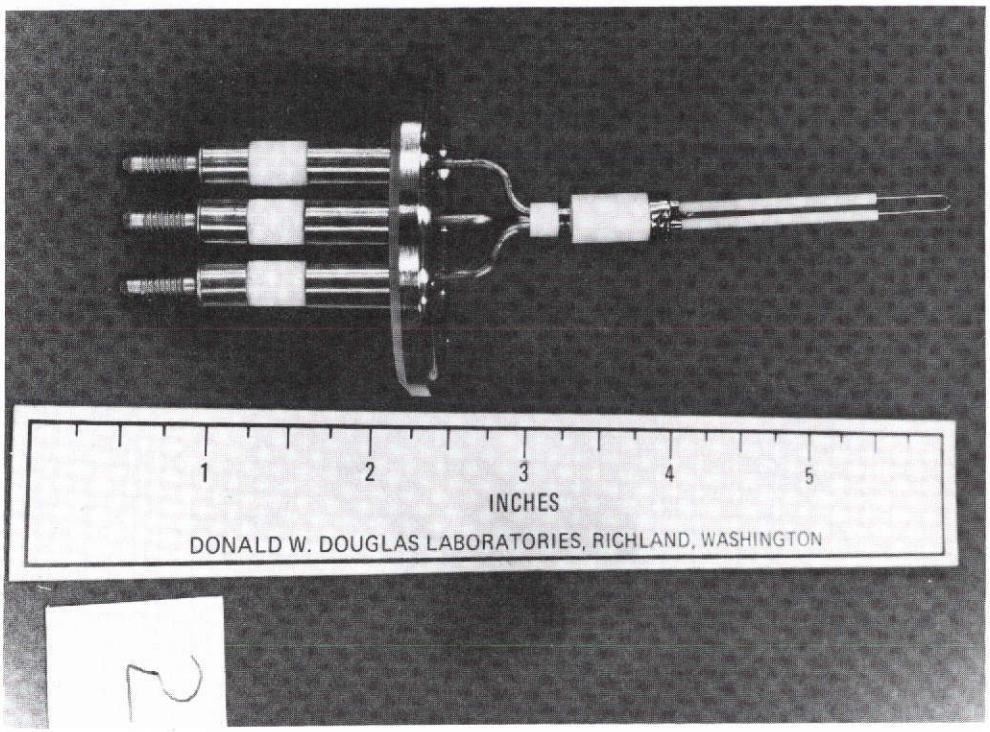

Figure 2-5. Configuration of Test Emitter

estimating the actual loop length. A greater uncertainty is contributed by the bore of the ceramic sleeve. If possible exposure to the plasma is considered to occur for a length into the sleeves equal to the bore radius, the exposed length increases by 1 mm. This contributes a ±2% uncertainty in estimating the electron emission area. The electron emission area of each emitter was taken as that contributed by the superficial exposed length and an additional length equal to the ceramic bore radius. The superficial length and area of each test emitter are summarized in Table 2-2.

PREPARATION OF MARCHUK TUBE (TASK 3)

The JPL-supplied Marchuk tube was disassembled for inspection as part of the preparation procedure. Regions of the ceramic liner and cathode insulators (Figure 2-6) had heavy metallic deposits and possibly other materials. These deposits apparently resulted from previous operation of the tube in argon at JPL.

Table 2-2

TEST EMITTER SUPERFICIAL EXPOSED LENGTH AND AREA

Emitter No.	Doping (a/o)	Superficial Length (cm)	Superficial Area (cm^2)
1	0.1	2.545	0.203
2	0.2	2.692	0.215
3	0.3	2.911	0.232
4	Ref	2.565	0.205

71-1505

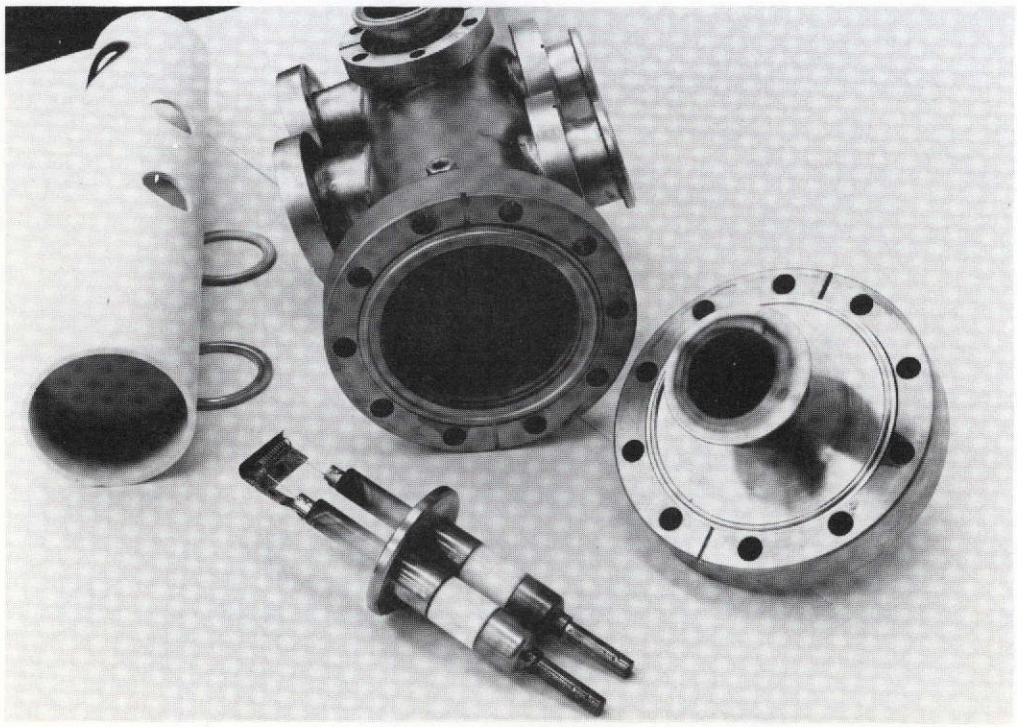

Figure 2-6. Disassembled Marchuk Tube

Treatment with aqua regia removed some deposits from the large ceramic liner. Remaining discoloration was removed by grinding with an alumina slurry. The tube was ultrasonically cleaned in four rinses of distilled water and air baked at 1300°K for 12 hours. Stainless steel assemblies were cleaned with Scotch-Brite and ultrasonically cleaned in Alconox and distilled water solutions. Three ultrasonic rinses with distilled water and one of reagent grade ethyl alcohol were followed by drying with a hot air gun. Two lucalox tubes surrounding the cathode were discarded because of contamination. The cathode was rebuilt with tantalum sheathing over the copper leads and an all-tantalum lead, filament, and shield assembly (Figure 2-7). A tantalum disc was also attached to cover the anode. All tantalum sheathing material was outgassed at 1800°K in a vacuum of approximately 10^{-4} N/m^2 ($\sim 10^{-6}$ torr).

The Marchuk tube was assembled with blank flanges and attached to a vacuum system pumped by a 400 liters-per-second titanium sublimation and a 30 liters-per-second Vac Ion system. Heating tape and insulation were

71-1670

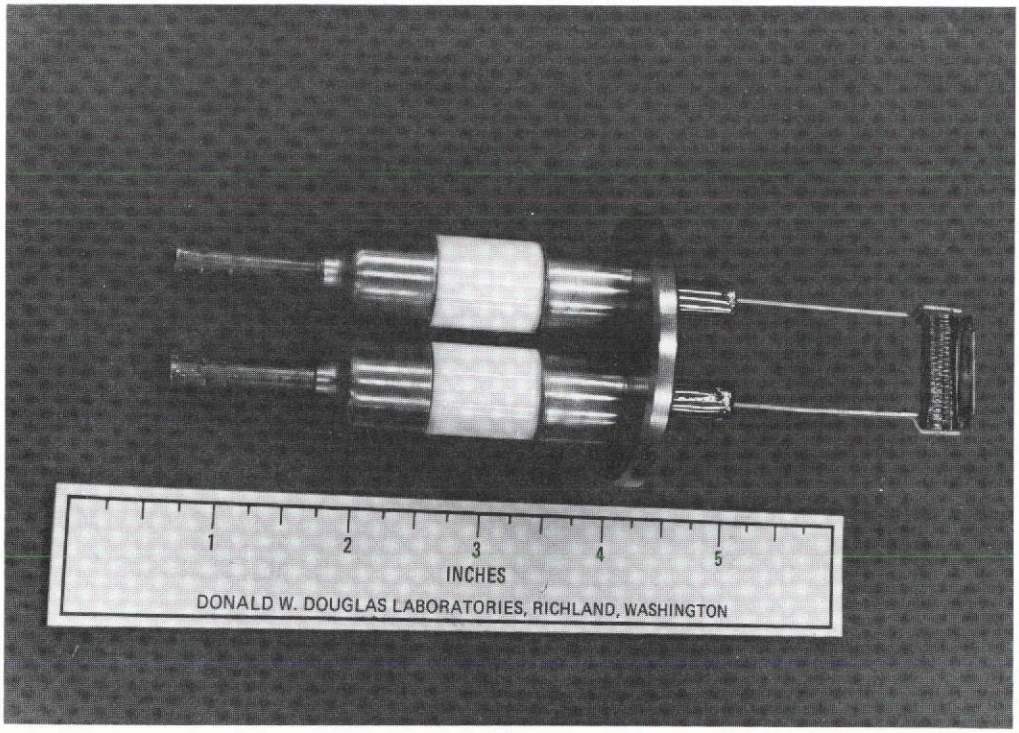

Figure 2-7. All-Ta Cathode Assembly with Ta Sheathing on Leadthroughs

attached and the tube was baked at 520°K (~250°C) for 96 hours and 620°K (~350°C) for 5 hours. After cooling, residual pressure was 8.8×10^{-7} N/m^2 (6.7×10^{-9} torr). The tube was connected through valving to a residual gas analyzer (Veeco Model GA-4). Water vapor was the predominant residual gas.

The blank flanges were replaced by the test emitter and cathode assemblies. The complete assembly was mounted on all-metal bakeable valves connected to the DWDL cesium still, residual gas analyzer, and associated vacuum systems (Figure 2-8). This arrangement is superior to charging the Marchuk tube with cesium and sealed operation as in conventional glass envelopes. The cesium still and Marchuk tube reflux cesium in a purification loop and are continuously pumped through an orifice by a Vac Ion system. A hot palladium foil permits the release of any hydrogen which may accumulate.

71-1725

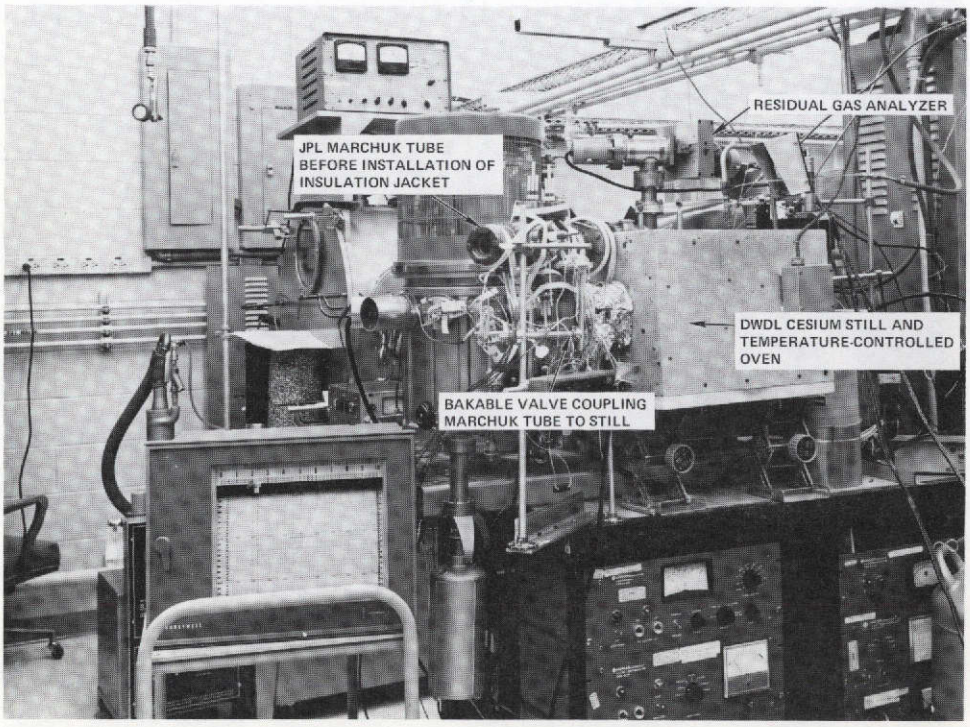

Figure 2-8. Arrangement of Marchuk Tube, Still, and RGA Before Installation of Insulation

Heater tapes and an insulation jacket were installed. The Marchuk tube was leak checked and baked at 620°K until minimum residual pressure was achieved. Pressures of less than 10^{-5} N/m^2 ($\sim 10^{-7}$ torr) and 10^{-7} N/m^2 ($\sim 10^{-9}$ torr) were recorded at 620° and 295°K respectively.

The Marchuk tube was reprocessed four times to these pressures after successive failure of tube components:

1. An Alberox insulator leaked with the tube under vacuum at room temperature. This was replaced by a new test emitter assembly.
2. The anode flange failed to seal during bake-out. Disassembly of the tube was necessary and a Varian flange replacement was welded in place.
3. A spot weld failed on the cathode filament under vacuum conditions but before cesium was admitted to the tube.
4. The most catastrophic event resulted from the development of a crack in the glass view port. This occurred at elevated temperature in cesium vapor and caused the burn-up of the cathode filament and heavy oxidation of the reference test emitter. Cesium hydroxide produced by reaction of cesium and water vapor from the air contaminated the cesium still. Refurbishment of the still, complete reprocessing of the Marchuk tube, and fabrication of four new test emitters were necessary. The view port was replaced by a Varian Model 954-5035 sapphire window assembly.

MARCHUK TUBE MEASURING CIRCUIT

Figure 2-9 identifies components of the measuring circuit. Test emitters were heated with half-wave rectified current. Emission current was measured during the "off" half-cycle to prevent disturbance of the signal by the heating current. An analog of heating current was provided by a Ballantine ac dc digital voltmeter. Emission current was synchronously switched to the y axis of an x-y plotter through a chopper driven by a Microdot square-wave generator. A 1-μf capacitor suppressed chatter in the x-y plotter. Emission current was sensed as a voltage across a precision shunt in the bias circuit. Emitter bias was provided by a Hewlett Packard 120-v, 1-amp power supply. Bias voltage was recorded on the x-axis of the x-y recorder. The bias was set so that the test emitter was more negative than the anode. At zero bias, therefore, the emitter was at anode potential and positive with respect to the plasma floating potential at the emitter point of insertion in the tube. Emitter current at zero bias results from electrons collected from the plasma.

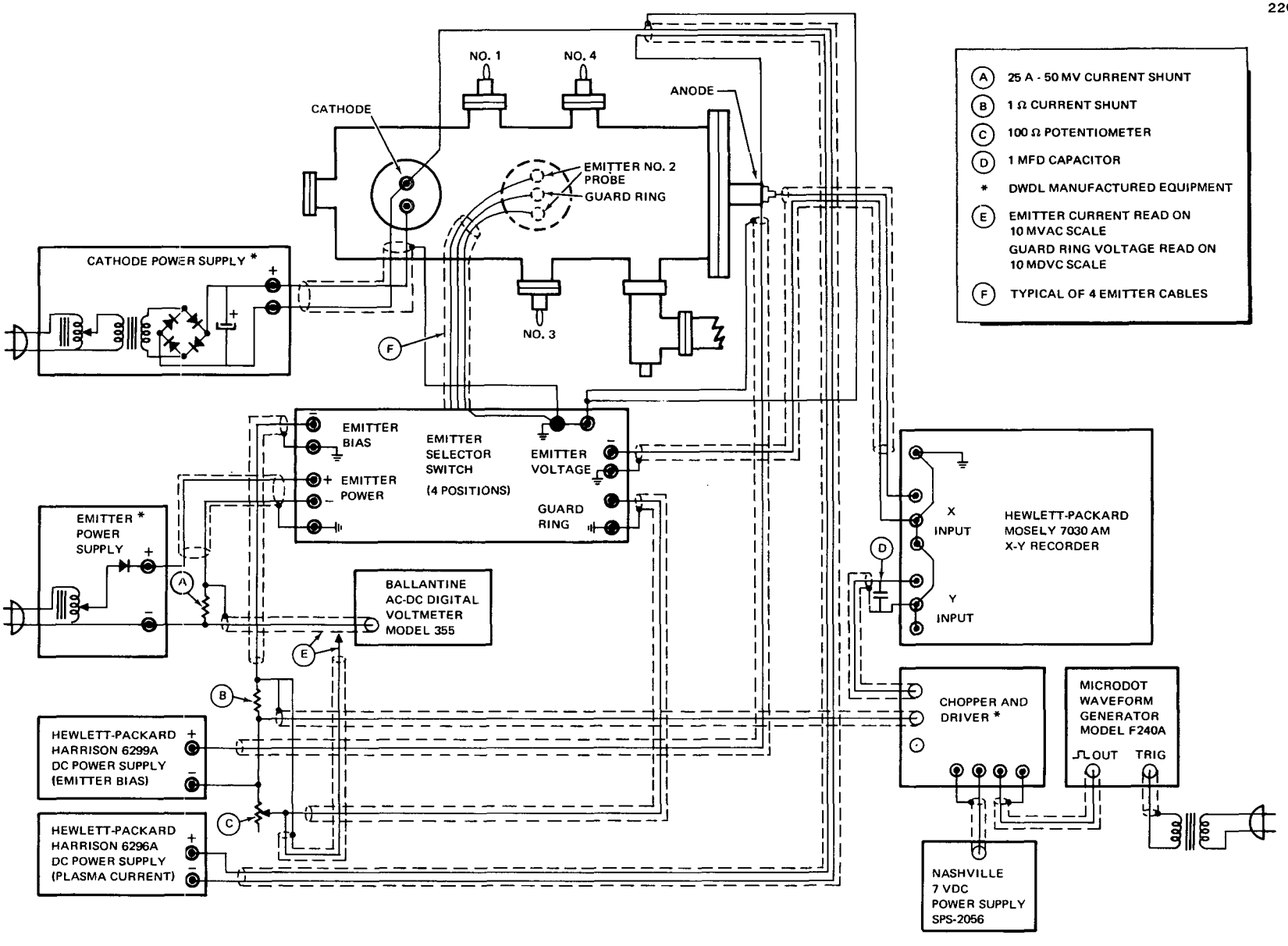

Figure 2-9. Marchuk Tube Measuring Circuit

As the probe becomes increasingly negative with respect to the anode, its potential bridges the floating potential of the plasma, and positive ion currents are measured. When the emitter is heated, electron emission adds to the plasma ion current. The knee of the curve indicates saturation emission after the ion current is subtracted. The method assumes no change of ion current caused by heating the test emitter.

The Marchuk tube was operated with the envelope electrically grounded. A Hewlett-Packard 60-v, 3 amp power supply supported the main discharge; the cathode was heated by direct current. A guard ring connection for each emitter was made through a potentiometer. This permitted adjustment of the guard ring potential to equal that of the test emitter.

TEST PROCEDURE (TASK 4 AND 5)

The Marchuk tube was heated to an average of 10°K above cesium reservoir temperature in the still. Additional heat was added to regions, such as lead-through flanges and valves, where cesium condensation was possible or apparent. A temperature calibration as a function of heater current to 1300°K was made for all test emitters without cesium in the tube, followed by complete calibration of the reference emitter to 2400°K. Temperatures were observed with an Epic micro-pyrometer (Model No. 3318) calibrated by a NBS-traceable standard, with a correction for view port transmissivity. Tantalum thermal emissivity data were taken from Reference 12 to calculate true emitter temperatures.

After the initial temperature calibration, cesium was admitted from the still at 413°K. Typical operating conditions of the main discharge were a 30-v anode/cathode potential difference with a discharge current of 50 ma. With each emitter at tube temperature, a plot of emitter current versus bias potential was made to indicate the positive ion current from the plasma. Each emitter was then heated, in turn, and emission characteristics were recorded over a range of temperature. Above 1300°K temperatures of the oxygen doped emitters were measured with the plasma extinguished after each emission measurement, until a complete calibration to 2400°K was obtained. This procedure was devised to achieve emission measurements and minimize loss of oxygen at high temperatures. Subsequently, temperatures

were inferred from the digital voltage analog of the emitter heater current. Calibration checks made throughout the experiment, showed repeatability to ±20°K at all temperatures. At the lowest temperature of interest, this represents, therefore, a worst case uncertainty of ±1.6% in temperature measurement. Emission measurements were made with emitter temperatures from 1035° to 2300°K in combination with cesium reservoir temperatures from 353° to 467°K. This reservoir temperature range corresponds to a cesium vapor pressure range from 2.6×10^{-2} to 8 N/m^2 ($\sim 2 \times 10^{-4}$ to 6×10^{-2} torr).

Test emitter work functions were calculated from the following derivative of the Richardson-Dushman equation,

$$\phi = -kT \ln \frac{J}{A_R T^2} \qquad (2\text{-}5)$$

where

ϕ is work function (ev)
$\frac{K}{e}$ is 8.63×10^{-5} ev. $°K^{-1}$
T is emitter temperature (°K)
J is emission current density ($A.cm^{-2}$)
A_R is the Richardson constant (120 $A.cm^{-2}.°K^{-2}$)

Calculated work functions were plotted as functions of the emitter temperature to cesium reservoir temperature (T/T_{Cs}) ratio, as described by Rasor and Warner (Reference 1).

Positive ion background currents were typically one to two orders of magnitude higher than are measured in conventional glass Marchuk tubes. Emission currents were generally indistinguishable from the ion current at emitter temperatures from 1400° to 1900°K. Emission from cesiated surfaces in the principal adsorption regime of interest was obscured by this effect. Oxygen depletion rates were, therefore, measured from 2140° to 2190°K to obtain emission current signals adequately distinguishable from the ion current background. The oxygen-doped emitters were operated, in turn, at these

temperatures until emission characteristics became identical to the reference electrode. Each emitter was then operated at 1273°K for approximately 3 hours to eliminate possible internal oxygen concentration gradients. Emission measurements at approximately 2150°K were repeated and compared with previous values.

After emission measurements and oxygen depletion tests were completed, the tube was disassembled and inspected. The oxygen-treated emitters and undoped electrode were sent to JPL for further analysis.

Section 3
DISCUSSION OF RESULTS

Despite the relatively large ion currents, the tendency of the tantalum bare work function to increase with oxygen-doping from 0.1 to 0.3 atomic percent was identified. The ion current background prevented observation of emission currents and oxygen depletion at 1800°K, and for conditions corresponding to T/T_{Cs} of approximately 3.0. An oxygen depletion effect was observed at an average temperature of 2165°K for each doped test emitter. A discussion of results and potentially valuable modifications in the Marchuk tube design are presented in this section.

DETERMINATION OF OXYGEN-DOPING LEVEL

A Millis Research (Model CSG-18) Color Step Gage was used as an independent measure of anodic film thickness formed on the test emitter wire stock. Table 3-1 compares the thickness derived from Equation 2-4 with that indicated by the color step gage.

The optical thickness indicated by the step gage was corrected by an average of 25 nm to account for phase shift at the Ta_2O_5/Ta interface (Reference 21). The anodic film thickness was calculated using an index of refraction for Ta_2O_5 of 2.45 (Reference 19). Uncertainty is contributed both by resolution of the color step gage (19 nm) and the range of phase shift correction (20 to 30 nm). However, for purposes of this study, the step gage showed that film thickness was established with acceptable accuracy during anodizing.

HARDNESS AND LATTICE PARAMETER COMPARISONS

The wire samples produced in this program were too small to contain a quantity of oxygen above the detection limit for gas analysis or neutron activation analysis techniques. An attempt was made to check oxygen concentration in the doped samples by hardness and lattice parameter measurements. Microhardness is plotted as a function of oxygen concentration in Figure 3-1.

Table 3-1

COMPARISON OF ANODIC FILM THICKNESS BY TWO METHODS OF MEASUREMENT

Required Doping (a/o)	Anodic Film Thickness Equation 2-4 (nm)	Step Gage (nm)	Uncertainty (%)
0.1	59	58 ±5	±8.6
0.2	118	118 ±5	±4.2
0.3	177	178 ±5	±2.8

A comparison with the results of Harrison (Reference 22) and Gebhardt and Seghezzi (Reference 23) shows a considerable range in absolute values of hardness. Present results, however, show an approximately linear dependence of hardness on oxygen concentration with a slope practically equal to the initial slope of referenced data. This suggests that oxygen doping proportional to the anodic film thickness had been achieved.

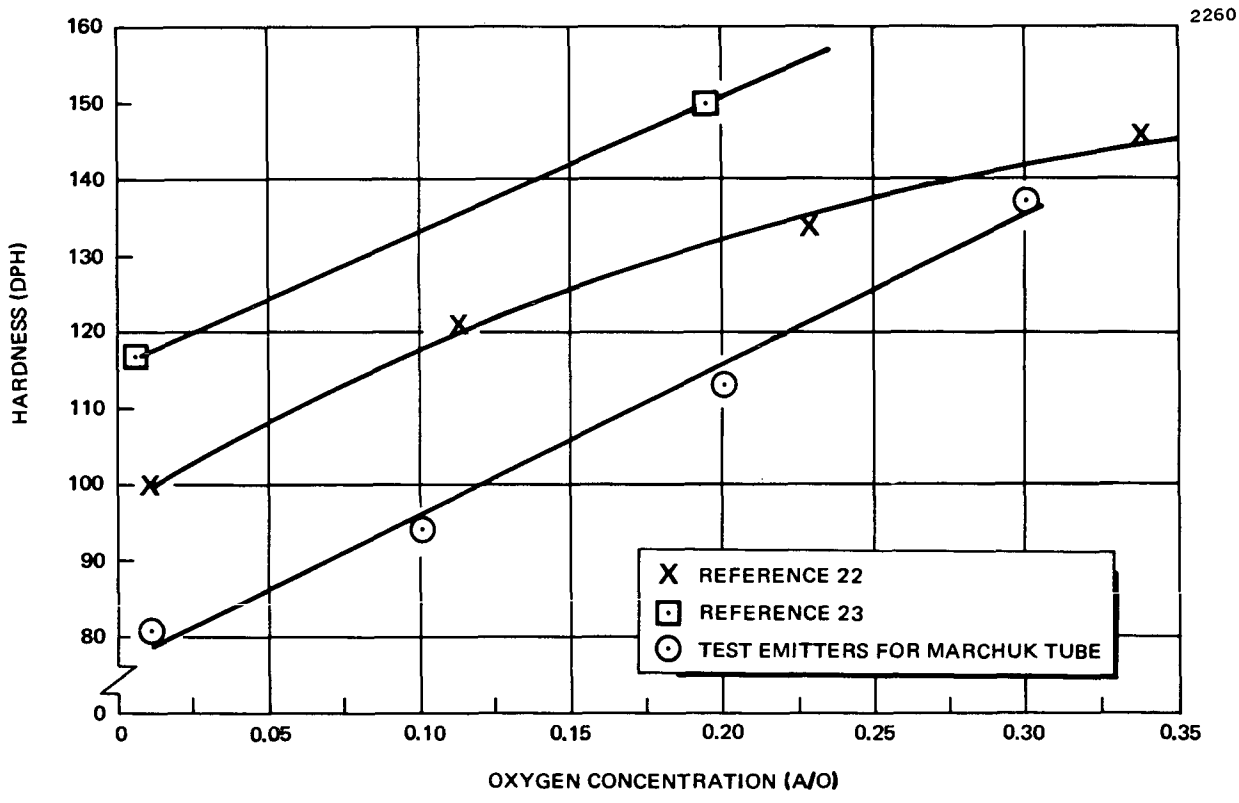

Figure 3-1. Hardness versus Oxygen Concentration

Four tantalum wire samples, one from each test emitter wire stock, were examined by x-ray diffraction to determine lattice parameters. Lattice parameter (A) is

$$A = b + mc \qquad (3\text{-}1)$$

where

b and m are constants

c is the oxygen concentration

Table 3-2 compares results of this study with data by Vaughan, et al (Reference 24) and Anuchkin, et al (Reference 25).

The results of this study are not in agreement with referenced data. The small sample surface and preferred orientation of the wires produced analytical conditions which were not ideal. However, a linear dependence lattice parameter on oxygen concentrations was indicated. The lattice parameter measurements corroborate the trend shown by hardness and together offer circumstantial evidence that oxygen-doping had been achieved in the desired ratios.

Table 3-2

COMPARISON OF TANTALUM LATTICE PARAMETER CONSTANTS

Parameter	Reference 24	Reference 25	This Study
b	3.3025	3.3030	3.3059
m	0.0040	0.0043	0.0023

WORK FUNCTION MEASUREMENTS (TASK 4)

A typical emission current versus bias potential plot is shown in Figure 3-2. The positive ion current is shown to be of the same order as two emission current traces. The magnitude of the ion current increased with cesium pressure and effectively obscured emission measurements in the range $3.0 < T/T_{Cs} < 4.0$. Work functions of the test emitters were calculated from emission measurements outside this range for several cesium pressures as indicated in Figures 3-3 through 3-6.

The obscuring effect of the positive ion current prevented work function measurements in the cesium adsorption range of interest for conventional thermionic emitters. The influence of oxygen doping, therefore, is inferred from the bare work function characteristics plotted generally for $T/T_{Cs} > 5$. By extrapolation of the cesium-bare emission to the cesium adsorption regime using the Rasor-Warner deviation, an estimation of the effect of doping can be made. Table 3-3 summarizes the bare work functions (ϕ_o) of the test emitters and the incremental change in work function ($\Delta\phi$) with respect to that of the pure tantalum reference emitter resulting from the doping measured at $T/T_{Cs} > 5$ and estimated at $T/T_{Cs} = 3$.

The relatively high ϕ_o of the reference emitter is attributed to preferred surface exposure of the 110 crystal plane. The work function of the 110 plane is 4.8 v (Reference 26) which tends to average upwards the normally accepted value of 4.1 v (Reference 12) for the polycrystalline material. Values of ϕ_o are reported with an error range accumulated by all uncertanties of calibration and measurement as described previously in Reference 8. Extrapolation of bare work function changes, indicate that the program goal of a reduction in work functions ≥ 0.3 v at $T/T_{Cs} \sim 3$ would be obtained with oxygen-doped tantalum in the range 0.2 to 0.3 a/o. In Table 3-3, bare work functions were derived from the initial three data collection runs with T_{Cs} of 413°, 397°, and 371°K, respectively. In subsequent runs, evidence accumulated to show partial outgassing of the dopant. Data scatter also increased with the number of high temperature exposures of the test emitters. Data for $T/T_{Cs} < 4$ is scattered to such an extent that no substantiation of the Rasor-Warner adsorption model can be made because of the small signal-to-positive ion current ratio. Scatter

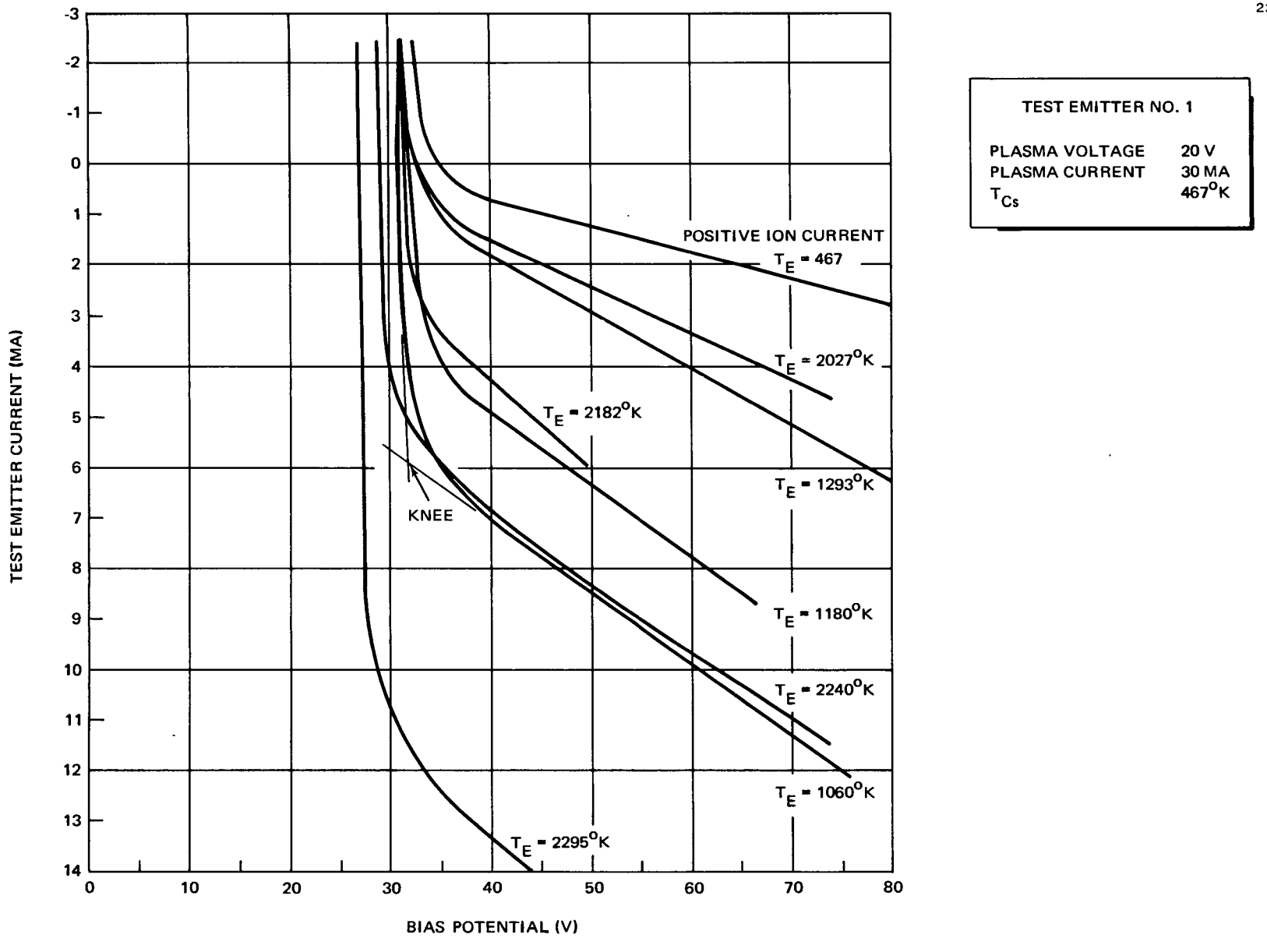

Figure 3-2. Typical Emitter Current versus Bias Potential

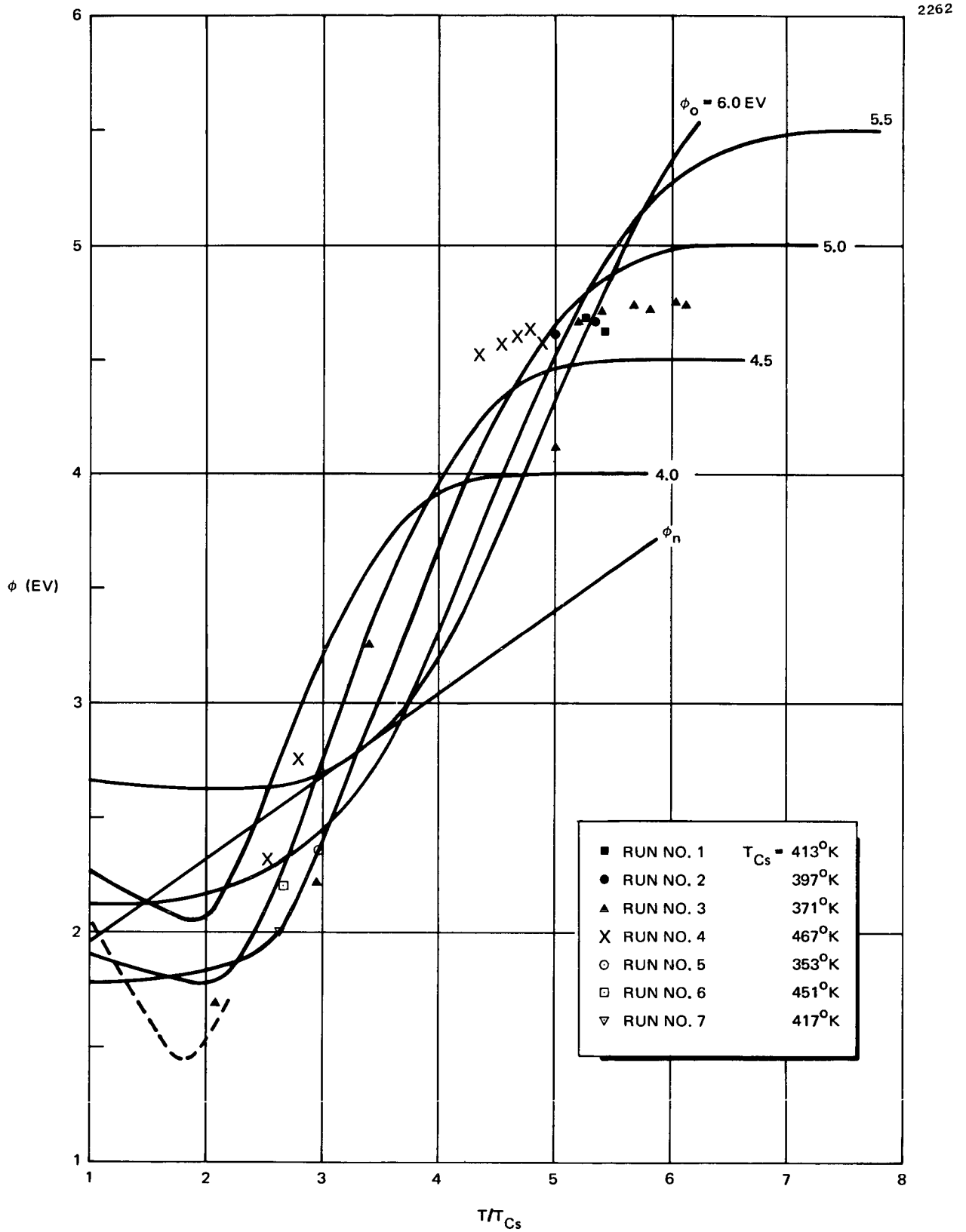

Figure 3-3. ϕ vs T/T_{Cs} Test Emitter No. 1 (oxygen doping 0.1 a/o)

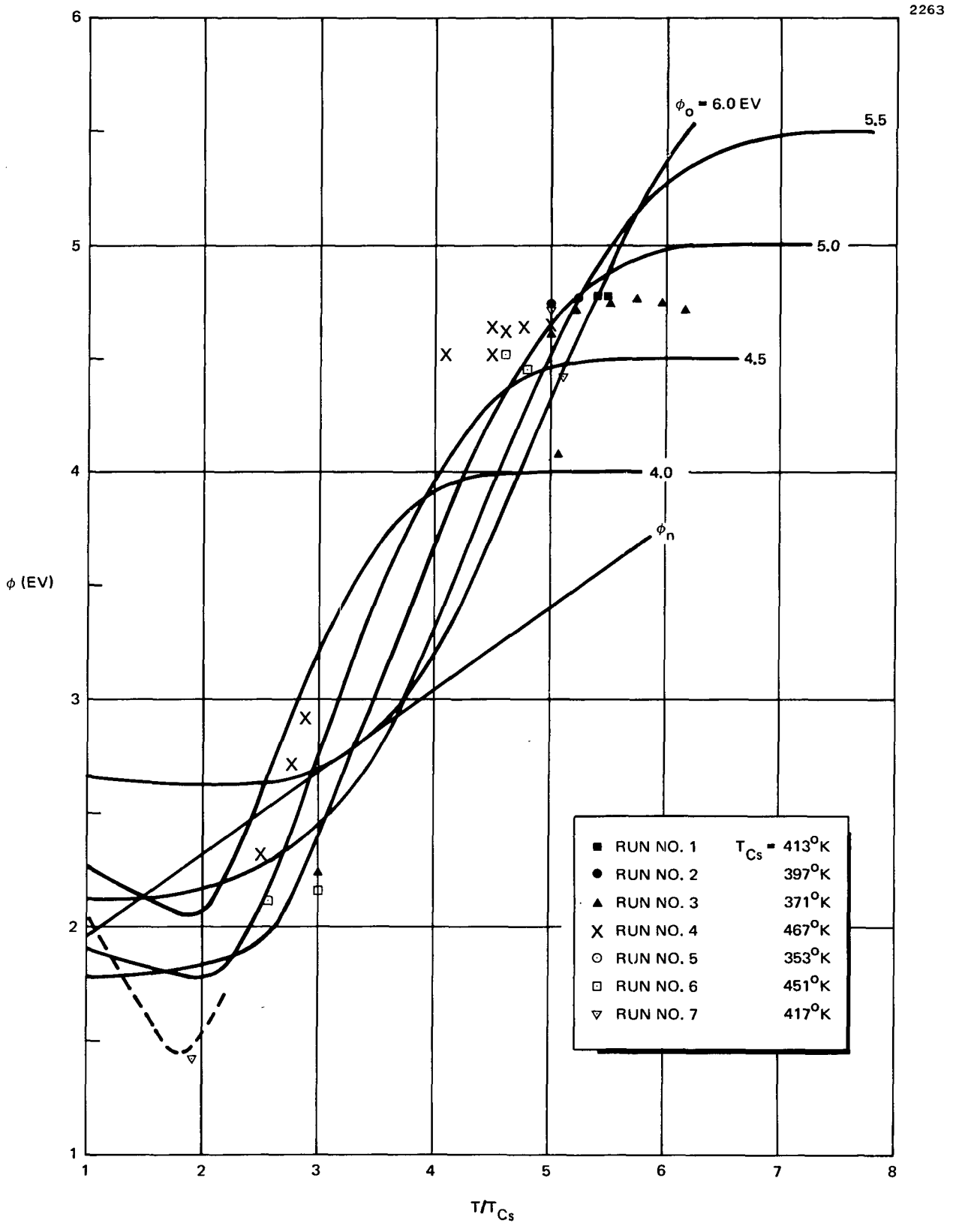

Figure 3-4. ϕ vs T/T_{Cs} Test Emitter No. 2 (oxygen doping 0.2 a/o)

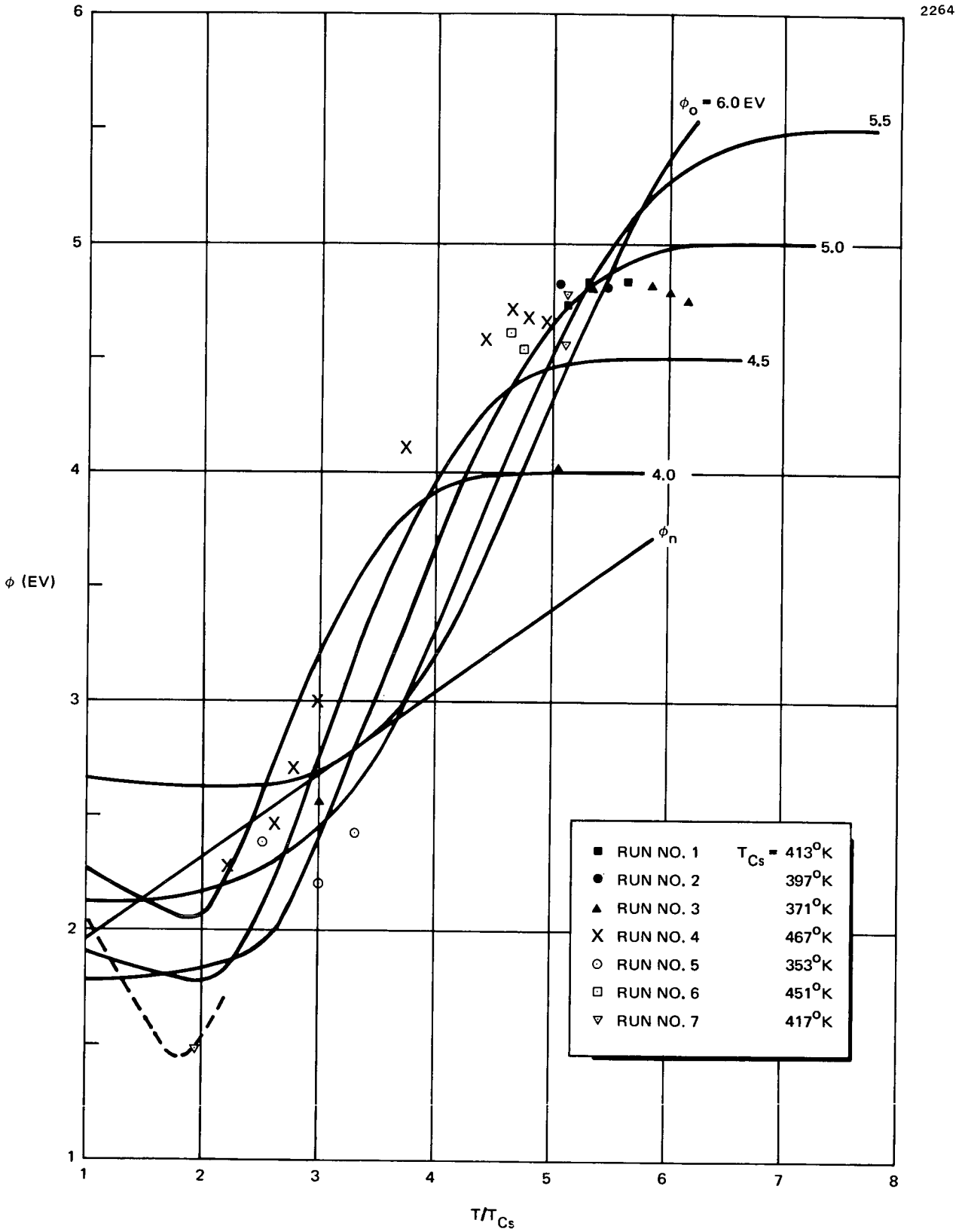

Figure 3-5. ϕ vs T/T_{Cs} Test Emitter No. 3 (oxygen doping 0.3 a/o)

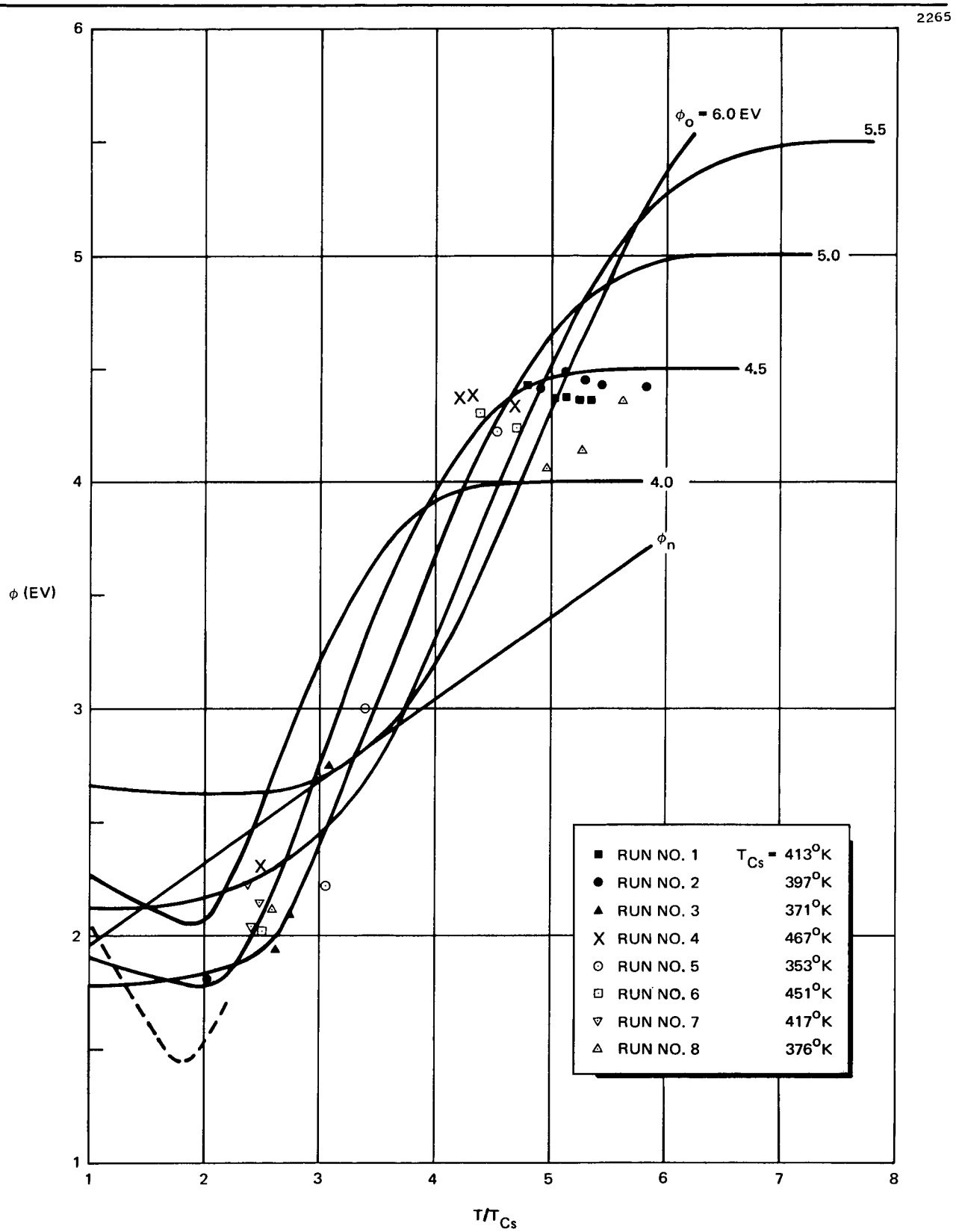

Figure 3-6. ϕ vs T/T_{Cs} Test Emitter No. 4 (tantalum reference electrode)

Table 3-3

COMPARISON OF TEST EMITTER WORK FUNCTIONS

Initial Oxygen Doping (a/o)	ϕ_o (ev)	ϕ_o at T/T_{Cs} $\Delta 5$ (ev)	Estimated $\Delta\phi$ at $T/T_{Cs} = 3$ (ev)
0 (Reference)	4.38 ±0.05	0	0
0.1	4.75 ±0.05	0.37	-0.27 ±0.10
0.2	4.78 ±0.05	0.40	-0.29 ±0.10
0.3	4.82 ±0.05	0.44	-0.33 ±0.10

is also to be found in the relatively large signal-to-background ratio domain at work function minima. In this region, DWDL (Reference 6) has shown a highly structured characteristic dependent both on emitter temperature and the T/T_{Cs} ratio. The narrow range of available temperatures providing adequate resolution of the emission current prevented work function mapping in this region. Nevertheless a trend to lowered work function minima (dashed line) is indicated as a consequence of oxygen doping, in general agreement with experience reported in Reference 6.

Other data points, notably those of Run No. 3 and 4, are totally outside the expected envelope of curves based on the Rasor-Warner cesium-adsorption models. Points to the left of accepted characteristics may result from cesium arrival rates in the Marchuk tube being different from those inferred from the liquid reservoir temperature. Tube temperatures were generally held within 10°K of still reservoir but bakable valves and emitter flanges were run to 50°K higher in temperature to prevent cesium condensation. Data showing unexpected low work function at $T/T_{Cs} > 4$ is attributed to cesium ion trapping by the ion sheath potential in the surface region of test emitters. This effect provides cesium coverages larger than those calculated from the T/T_{Cs} equilibrium values.

OXYGEN DEPLETION TESTS (TASK 5)

The change in work function of each emitter was measured with time as an indication of depletion in oxygen doping. Feasibility of oxygen-doped tantalum as a high temperature thermionic emitter is dependent on a low oxygen emission

rate at operating temperatures. An initial goal for work function stability (i. e., no significant change in oxygen concentration) of 10,000 hours at 1800°K has been identified for this program. To produce significant work function changes within the program schedule and to also provide an emission current level distinguishable from the ion background current, test emitters were observed for approximately 9 hours with T_{Cs} = 376°K and temperatures from 2140° to 2190°K. Figure 3-7 summarizes the work function history of the test emitters.

The period -5000 to 0 seconds in Figure 3-7 represents changes occurring during the time work function measurements were made to establish characteristics in Task 4. The initial influence of oxygen doping is clearly demonstrated by the monotonic increase in bare work function. The work functions of all doped emitters are shown to have decreased during Task 4 operations, which is indicative of oxygen loss. A corresponding increase in work function of the reference emitter is interpreted as the result of oxygen absorption. A fraction of the outgassed oxygen from the doped emitters would be available for

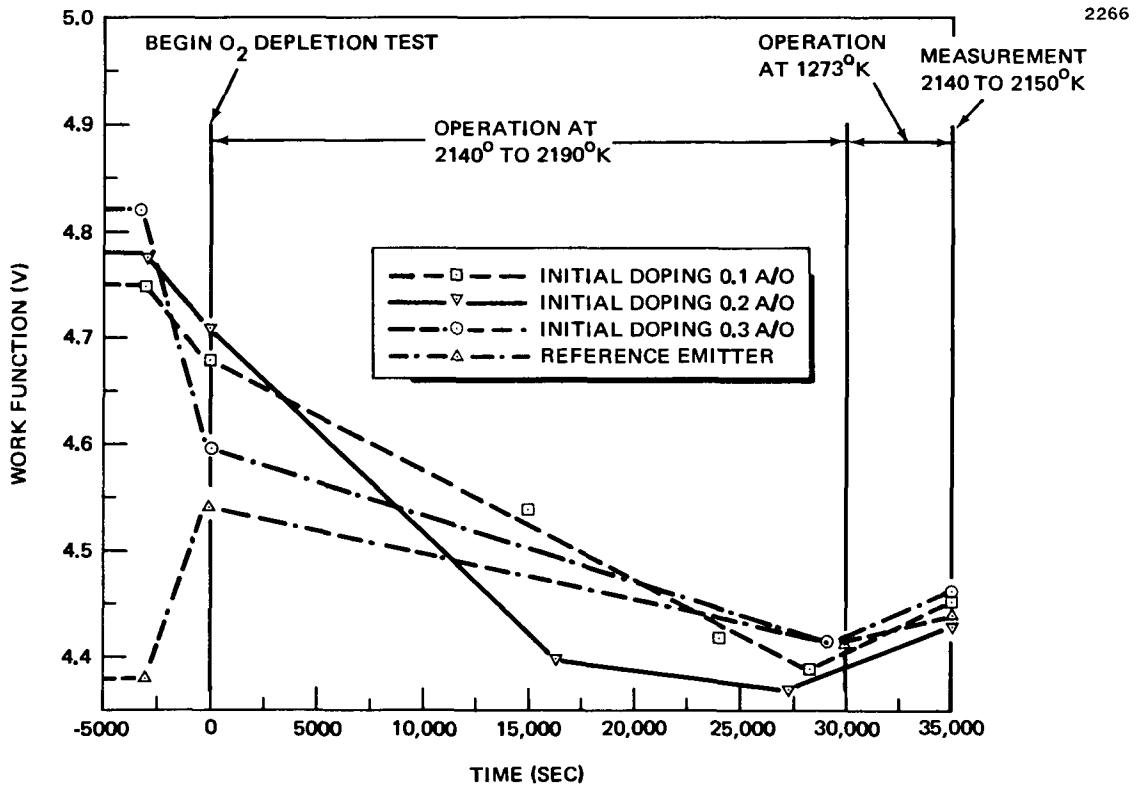

Figure 3-7. Bare Work Function of Test Emitters

reabsorption by the undoped reference emitter. All emitters appear, therefore, to be partially oxygen-doped at the beginning of the depletion test. Operation at elevated temperatures was shown to deplete all emitters to levels approaching that of the original condition of the vigorously outgassed reference electrode. Ratios of T/T_{Cs} ranged from 5.7 to 5.8, and therefore, all work functions were measured without coadsorption of cesium.

After the depletion tests, all emitters were heated to 1273°K for approximately 3 hours. This duplicated the conditions under which dissolution of the anodic films had been achieved. The purpose of this operation was to equilibrate possible oxygen concentration gradients left in the wire. These gradients, after the high temperature depletion test would, if they existed, be related inversely to the distance from the wire center line. Test emitter work functions were again checked after the 1273°K period, at temperatures from 2140° to 2150°K. The work functions of all emitters increased and closely grouped from 4.43 to 4.46 ev, without order, based on previous levels. This provides evidence that residual oxygen had been effectively outgassed during the depletion test, and that free oxygen in the tube had also been readsorbed during the 1273°K exposure.

The outgassing kinetics of gas-metal-solid solutions have been summarized by Fromm (Reference 27). For the Ta-O system, the residual concentration of oxygen (ϕ) is related to outgassing time (t) and temperature by

$$\log \frac{c}{c_o} = -1.7 \times 10^{9} \frac{at}{\rho v} \exp\left(-6.65 \times 10^{4}/T\right) \qquad (3\text{-}2)$$

where

c_o = oxygen concentration for t = 0 (a/o)
a = surface area (cm^2)
ρ = density ($g \cdot cm^{-3}$)
v = volume (cm^3)

This equation is valid for specimens <1 mm in diameter, T > 1650°K, and c_o < 0.5 a/o, and therefore, is applicable to the test emitter in this study. Using the depletion test conditions t ~ 3×10^4 seconds, T ~ 2165°K results in a value of $c/c_o \sim 10^{-22}$. However, the residual oxygen in the gas phase should prevent outgassing to this extreme.

Steady state conditions with oxygen in the gas phase are given by (Reference 27)

$$\log c = \log P_{O_2} - 2.69 + 15,000/T \qquad (3\text{-}3)$$

where

P_{O_2} is oxygen pressure (torr)

Assuming a 10^{-7} N/cm^2 ($\sim 10^{-9}$ torr) oxygen partial pressure in the Marchuk tube, the equilibrium value of $c \sim 10^{-5}$ a/o is calculated.

This study generated too few data points to substantiate the kinetics of oxygen loss quantitatively. However, at the emitter temperature of interest ($\sim$1800°K) for the application of oxygenated tantalum to high temperature converters, oxygen loss is controlled by the kinetics in Equation 3-2 where the a/v ratio is a controlling variable. In this study, the a/v ratio of the test emitters was approximately 157 cm^{-1}. In a practical converter, ratios of one or two orders less would be feasible. If it is assumed that Equation 3-2 is not invalidated by substituting a/v = 2 cm^{-1}, T = 1800°K and t = 10,000 hr, Equation 3-2 yields $c/c_o = 0.22$. Therefore, an emitter doped to approximately 1 a/o would degrade to 0.22 a/o after 10,000 hours operation. Table 3-3 shows that this degradation could be tolerated and that the emitter would still provide a surface with a $\Delta\phi \geq -0.3$ ev at $T/T_{Cs} \sim 3$.

POST-OPERATION EXAMINATION OF MARCHUK TUBE

The experiment was disassembled after several days operation with the cesium still at 295°K. The Marchuk tube was heated to 600°K to drive residual cesium into the still system. After cooling, the tube was removed from the test station and components were inspected. Tantalum parts exhibited a blue interference coloration of varying intensity, suggesting thin-film deposition of some material. This may be attributed to condensation of a volatile tantalum oxide species evolved during test emitter operation at >2000°K. Test emitter specimens were sent to JPL for further analysis.

RECOMMENDED MARCHUK TUBE MODIFICATIONS

The high positive ion currents measured suggest improvements to the Marchuk tube configuration. Ion densities on the order of 5×10^{12} cm^{-3} were calculated from ion currents collected by the test emitters and cesium vapor temperature. This ion density is on the expected order and agrees with measurements by Shimada and Cassell with argon in the same Marchuk tube. It is possible that the metal envelope promotes higher plasma leakage to the walls in the region of the test emitter ports, than that in the glass envelope configuration and ion currents are intercepted by the leads attached to the test emitter. It is recommended that additional shielding be added in the test emitter port for the Phase II and Phase III studies. Further reduction of the ion current should be achieved by a shorter exposed test emitter length and by offsetting the test emitter radially from the tube center line.

Section 4
CONCLUSIONS

The objectives of the Phase I program were achieved in essence, however, significant problems were encountered in the preparation and operation of the JPL metal/ceramic Marchuk tube. Measurement of probe temperature and estimation of emitter areas were achieved within the required range of accuracy.

Tantalum work functions were shown to increase monotonically with oxygen doping from 0.1 to 0.3 a/o. This effect was established in the cesium-bare region of the Rasor-Warner diagram describing the work function dependence on the T/T_{Cs} ratio for cesiated refractory metals. The emission from oxygen-doped test emitters was compared with that of a rigorously outgassed tantalum reference electrode to distinguish effects from contamination in the Marchuk tube. Extrapolation of work function data to $T/T_{Cs} \sim 3$ indicated achievement of the program goal with work function reduction ≥ 0.3 ev. This program provided the first opportunity to operate the JPL-built metal/ceramic Marchuk tube containing cesium vapor. Meaningful data was gained despite component failures on four occasions which caused shut-down of the experiment and refurbishment of the experimental apparatus. The metal/ceramic Marchuk tube showed a high positive ion current collection characteristic not found in conventional glass Marchuk tubes. This was roughly proportional to the cesium arrival rate and obscured emission currents associated with the linear portion of the Rasor-Warner cesium adsorption characteristic. As a result, work functions were not measured in the emitter operational regime of the conventional thermionic converter.

Oxygen depletion tests showed the decay of oxygen-enhanced work function to a level approximately equal to that of the reference tantalum electrode. The reference electrode showed some increase in work function which is interpreted to result from absorption of oxygen from species outgassed from other emitters. An approach to total depletion of oxygen doping was achieved in approximately 9 hours with temperatures ranging from 2140° to 2190°K.

Kinetic consideration of oxygen loss showed that practical emitters would retain useful quantities of oxygen at end-of-life after 10,000 hours operation at 1800°K. Initial doping levels of approximately 1 a/o would decay to 0.22 a/o after this exposure. This reduced doping level would still provide a favorable work function reduction compared to that of pure tantalum in the typical operational regime of a plasma-mode converter.

Inspection of components after disassembly of the experiment showed thin film interference colors on exposed tantalum surfaces. Coloration was apparent on exposed portions of test emitters; metallic luster was observed on regions shielded by ceramic tubes. The films are most probably tantalum oxides formed by condensation of subliming tantalum oxide species from the test emitters.

Effort recommended for Phase II and III includes design modifications to reduce the positive ion background current. Additional shielding in the test emitter ports, reduced test emitter exposed length, and emitter positions offset from the tube centerline are planned. Operation of the tube connected to a continuously pumped cesium still was successfully accomplished in the Phase I effort and will be continued in the Phase II and III programs.

Section 5

BIBLIOGRAPHY

Oxidation of Tantalum

E. A. Gulbransen and R. F. Andrew. Reactions of Zirconium, Titanium, Columbium, and Tantalum with the Gases, Oxygen, Nitrogen, and Hydrogen at Elevated Temperatures. J. of Electrochem. Soc. 96, 364 (1949).

E. A. Gulbransen and K. F. Andrew. Reactions of Columbium and Tantalum with Oxygen, Nitrogen, and Hydrogen. Journal of Metals, March 1950, Transactions AIME, Vol. 188.

J. T. Waber, G. E. Sturdy, E. M. Wise, and C. R. Tipton, Jr. A Spectrophotometric Study of the Oxidation of Tantalum. J. Electrochem. Soc., 99, 121 (1952).

E. Gebhardt and H. Preisendanz. Über die Löslichkeit von Sauerstoff in Tantal und die damit verbundenen Eigenschaftsanderungen. Z. Metallkde, 8, 560 (1955).

D. A. Vermilyea. The Oxidation of Tantalum at 50° - 300°C. Acta Metallurgica, Vol. 6, March 1958.

E. Gebhardt and H. Seghezzi. Investigations in the Tantalum-Oxygen System. Z. Metallkde, 50, 248 (1959).

N. Norman, P. Kofstad, and O. J. Krudtaa. Metallic Oxide Phases of Niobium and Tantalum. J. Less-Common Metals, 4, 125 (1962).

P. G. Shewmon. Diffusion in Solids. McGraw-Hill Book Company, New York, N. Y., 1963.

C. L. Standley and L. I. Maissel. Some Observations on Conduction through Thin Tantalum Oxide Films. J. Appl. Phys., 35, 1530 (1964).

C. G. Dunn and H. F. Webster. Development of a (110) Preferred Orientation in Rolled and Annealed High-Purity Tantalum. Trans. Metallurg. Soc. AIME, 230, 1567 (1964).

T. E. Tietz and J. W. Wilson. Behavior and Properties of Refractory Metals, Stanford University Press, Stanford, Calif., 1965.

J. Neibuhr. Die Niederen Oxide Des Tantals. J. Less-Common Metals, 10, 312 (1966).

J. Stringer. The High-Temperature Oxidation of Tantalum Single Crystals. J. Less-Common Metals, 12, 301 (1967).

M. Parkman, R. Pape, R. McRae, D. Brayton, and L. Reed. Solubility and Diffusion of Oxygen in Tantalum. NASA CR-1276.

M. D. Ketchum, C. A. Barrett. The Contamination of Refractory Metals by Oxygen, Water Vapor, and Carbon Monoxide. Final Report, NAS-3-8518, June 1969.

C. A. Steidel and D. Gerstenberg. Thermal Oxidation of Sputtered Tantalum Thin Films Between 100° and 525°C. J. Appl. Phys., 40, 3828 (1969).

E. A. Gulbransen. Thermochemistry and the Oxidation of Refractory Metals at High Temperature. Corrosion, 26, 19 (1970).

P. H. G. Draper and J. Harvey. The Structure of Anodic Films--I. An Electron Diffraction Examination of the Products of Anodic Oxidation on Tantalum, Niobium, and Zirconium. Acta Metallurgica, 11, 873 (1963).

R. Pape, L. Reed, and R. McRae. An Investigation of Solubility and Diffusion of Oxygen in Refractory Metals. Third Quarterly Report NASA-CR-54648 January-March 1966.

Anodization of Tantalum

L. Young. The Determination of the Thickness, Dielectric Constant, and Other Properties of Anodic Oxide Films on Tantalum from the Interference Colours. Proc. Royal Soc. A., 244, 41 (1958).

A. R. Bray, P. W. M. Jacobs, and L. Young. Photo-Induced Growth of Anodic Tantalum Pentoxide Films. J. Nuclear Materials, 4, 356 (1959).

G. Amsel and D. Samuel. The Mechanism of Anodic Oxidation. J. Phys. Chem. Solids, 23, 1707 (1962).

D. M. Smyth, G. A. Shirn, and T. B. Tripp. Heat-Treatment of Anodic Films on Tantalum. J. Electrochem. Soc., 110, 1264 (1963).

C. L. White and W. E. Patterson. Conductance During Anodic Oxidation of Tantalum and Niobium Films. J. Electrochem. Soc., 111, 1336 (1964).

D. M. Smyth. The Heat-Treatment of Anodic Oxide Films on Tantalum. J. Electrochem. Soc., 114, 723 (1967).

G. J. Korinek. The Activation Energies of Conduction in Tantalum Anodic Films. Electrochemical Technology, 6, 108 (1968).

J. F. O'Hanlon and W. B. Pennebaker. Negative Ion Extraction from the Plasma During Anodization in the dc Oxygen Discharge. Appl. Phys. Letters, 18, 554 (1971).

Section 6
REFERENCES

1. N. S. Rasor and C. Warner. Correlation of Emission Processes for Adsorbed Alkali Films on Metal Surfaces. J. Appl. Phys. Vol 35, No. 9, 2589, September 1964.

2. D. Ernst and C. Pezaris. Life Test on Four Electrically-Heated Thermionic Diodes with Fluoride Vapor-Deposited Tungsten Emitters. Thermo Electron Corporation Report No. TE 4086-13-70, June 1969.

3. J. D. Levine. Oxygen as a Beneficial Additive in Cesium Thermionic Energy Converters. J. Appl. Phys. Vol 38, No. 2, 892, February 1967.

4. R. Langpape and A. Minor. Work Functions of Polycrystalline W and Re in an Atmosphere of Cesium and Oxygen. Proc. Second International Conference on Thermionic Electrical Power Generation, Stresa, Italy, May 1968.

5. I. Langmuir and K. H. Dingdon. Proc. Roy. Soc. (London) A 107, 61, (1925).

6. M. S. Mayer, et al. Optimization of the Quasi-Vacuum Mode Thermionic Converter. McDonnell Douglas Paper WD-1472, presented at the 1970 Thermionic Conversion Specialist Conference, Miami Beach, Florida, October 1970.

7. M. S. Gottlieb, et al. Heat Diode Converter. Air Force Systems Command Report ASD-TDR-62-1082, May 1963.

8. S. S. Luebbers and J. G. DeSteese. Oxygen Effects in Tantalum Emitters. Proc. 1968 Thermionic Conversion Specialist Conference, Framingham, Massachusetts, October 1968.

9. P. M. Marchuk. Trudy Inst. Fiz. Ak. Nauk. Ukrain 7, 17, 1956.

10. K. Shimada and P. L. Cassell. Plasma-Anode Tube in Metal/Ceramic Envelope. IEEE Record of 1970 Thermionic Conversion Specialist Conference, Miami Beach, Florida, October 1970.

11. J. M. Houston and P. K. Dederick. Thermionic Emission of Thermionic Converter Collector Materials in Cesium Vapor. Record of the 1964 Thermionic Conversion Specialist Conference, Cleveland, Ohio, October 1964.

12. W. H. Kohl. Handbook of Materials and Techniques for Vacuum Devices. 1967 Edition, Reinhold Publishing Corporation.

13. S. Dushman. Scientific Foundations of Vacuum Technique. John Wiley and Sons, Inc.

14. E. Gebhardt, E. Fromm, and D. Jakob. Vorgänge bei der Entgassung von Niob und Tantal, Metals for the Space Age, Plansee Proc. 1964, Springer Verlag.

15. P. L. Worledge and D. White. Controlled Oxidation of Tantalum and Aluminum in a Radio-Frequency-Excited Glow Discharge. Brit. J. Appl. Phys., 18, 1337 (1971).

16. F. Vratny. Tantalum Oxide Films Prepared by Oxygen Plasma Anodization and Reactive Sputtering. J. Amer. Ceram. Soc., 50, 283 (1967).

17. G. Amsel, C. Cherki, G. Feuillade, and J. P. Nadai. The Influence of the Electrolyte on the Composition of 'Anodic Oxide Films' on Tantalum. J. Phys. Chem. Solids 30, 2117 (1969).

18. J. J. Randall, Jr., W. J. Bernard, and R. R. Wilkinson. A Radiotracer Study of the Composition and Properties of Anodic Films on Tantalum and Niobium. Electrochimica Acta, 10, 183 (1965).

19. D. A. Vermilyea. The Kinetics of Formation and Structure of Anodic Oxide Films on Tantalum. Acta Metallurgica, 1, 282, 1953.

20. R. W. Powers and M. V. Doyle. Diffusion of Interstitial Solutes in the Group B Transition Metals. J. Appl. Phys., 30, 514 (1959).

21. W. Gasko of Millis Research. Private communication.

22. R. W. Harrison. SNAP 8 Refractory Boiler Development-Corrosion of Oxygen Contaminated Tantalum in NaK. General Electric Co. Report NASA CR-1850, July 1971.

23. E. Gebhardt and H. D. Seghezzi. Neuere Erkenntnisse in System Tantal-Sauerstoff. Plansee Proc. 1958.

24. D. A. Vaughan, O. M. Stewart and C. M. Schwartz. Determination of Interstitial Solubility Limit in Tantalum and Identification of the Precipitate Phases. Trans. Met. Soc. AIME 221, 937 (1961).

25. A. M. Anuchkin, A. K. Volkov, I. N. Kidin, T. M. Rozhnova, and M. A. Shtremel. Measurement of the Concentration of Oxygen Dissolved in Tantalum. Izv. Vyssh. Ucheb. Zaved (1970). English translation ORNL-tr-2479.

26. M. H. Richman. The Work Function and Surface Energy in BBC Metals. Trans. of the ASM 60, 7, 9, (1967).

27. E. Fromm. Gas-Metal Reactions of Refractory Metals at High Temperature in High Vacuum. J. Vac. Sci. and Tech. 7, 100 (1971).

Appendix A
CERTIFICATION OF TANTALUM WIRE STOCK

The chemical report on annealed tantalum wire 0.01 inch diameter x spool length Production No. W83986 Lot No. MG-87 from Fansteel Inc., Metals Division, is as follows.

Element	Concentration (ppm)
C	10-
O	25
N	25
H	5-
W	100
Cb	270
Zr	10-
Mo	10-
Ti	10-
Fe	10-
Ni	10-
Si	10-
Mn	10-
Ca	10-
Al	10-
Cu	10-
Sn	10-
Cr	10-
V	10-
Mg	10-
Ta	Bal.

Appendix B
DIFFUSION EQUATION SOLUTION-SLAB GEOMETRY

For a constant diffusion coefficient D, Fick's law in one dimension is

$$\frac{\partial c}{\partial t} = D \frac{\partial^2 c}{\partial x^2}$$

where c = concentration in cm^{-3}.

Utilizing the technique of separation of variables:

$$\frac{1}{DT}\frac{dT}{dt} = \frac{1}{X}\frac{d^2X}{dx^2} = -\lambda^2$$

The differential equation in time has, by inspection, the solution

$$T = \alpha \exp(-\lambda^2 Dt)$$

Where λ is a real number determined by solving the differential equation in x and applying boundary conditions. This spatial dependence is, by inspection,

$$X(x) = A_o \sin \lambda x + B_o \cos \lambda x$$

so that the total solution in its most general form is

$$c(x, t) = \sum_{N=1}^{\infty} (A_n \sin \lambda x + B_n \cos \lambda x) \exp(-\lambda^2 Dt) + C\infty$$

C_∞ is the concentration at infinite time.

A, B, and λ are determined as follows: The physical situation of interest is one where essentially a Dirac delta of solute is deposited on one surface of the slab. This solute, in amount (Q cm^{-2}) will be allowed to diffuse through

the sample, and at some time, t_f, the concentration will be essentially flat, i.e., $c(x, t > t_f) \simeq Q/L$, where L is the slab thickness. The concentration as a function of time at both surfaces is desired for microhardness correlations, and the time, t_f, for estimating diffusion time and temperature necessary for a uniform composition. The slab solution for t_f, where L equals the experimental wire diameter, will also give a conservative time-temperature estimate for a cylinder.

Assuming conservation of the solute, the derivative of concentration with respect to position must be zero for all time at x = 0 and x = L. For this to be true, A_n must equal 0, and

$$\lambda n = \frac{n\pi}{L}$$

The solution has the form

$$(x, t) = \sum_{N=1}^{\infty} B_n \cos\left(\frac{n\pi x}{L}\right) \exp\left(-\left(\frac{n\pi}{L}\right)^2 Dt\right) + Q/L$$

Proceeding by standard operations, the coefficients, B_n, are

$$B_n = \frac{2}{L} \int_o^L c(x, o) \cos(n\pi x/L) dx$$

If c(x, o) is defined as a one-sided Dirac function at zero, from the definition of that function, the integral, for all n, is essentially

$$B_n = \frac{2Q}{L},$$

which gives the final solution to the diffusion equation as

$$c(x, t) = \frac{Q}{L}\left[1 + 2 \sum_{N=1}^{\infty} \cos(n\pi x/L) \exp\left(-\left(\frac{n\pi}{L}\right)^2 Dt\right)\right]$$